International Geology Review, Vol. 48, 2006, p. 725–741.

Baimazhai, Yunnan Province, China: A Hydrothermally Modified Magmatic Nickel-Copper-PGE Sulfide Deposit

XUESHU ZHANG,

Kunming University of Science and Technology and Yunnan Nonferrous Metals Geological Bureau, 650051, Kunming, Yunnan Province, People's Republic of China

FRANCO PIRAJNO,[1]

Geological Survey of Western Australia, 100 Plain Street, East Perth WA 6004, Australia

DEXIAN QIN, ZHUGUO FAN, GUANLIANG LIU,

Kunming University of Science and Technology, 650051, Kunming, Yunnan Province, People's Republic of China

AND HONG NIAN

Yunnan Nonferrous Metals Geological Bureau, 650051, Kunming, Yunnan Province, People's Republic of China

Abstract

The Baimazhai Ni-Cu-PGE (platinum-group-elements) sulfide deposit, southeast Yunnan Province, is hosted in mafic-ultramafic intrusions of the Permian Emeishan large igneous province, with which it is temporally and genetically related. The typical orthomagmatic sulfide ores of the Baimazhai deposit locally exhibit peculiar textural features, and are intimately associated with hydrothermal minerals such as biotite, amphibole, and chlorite. This suggests that magmatic sulfide ores were subjected to hydrothermal alteration and subsequent redistribution, resulting in enrichment in Cu, Pd, and Au. Whole-rock ^{40}Ar-^{39}Ar age data yielded plateau ages of about 160–170 Ma, at odds with the established Permian age of the host intrusions and the Emeishan large igneous province. We interpret these younger ages as due to thermal resetting during post-Permian tectonothermal events such as the Jurassic Cretaceous Yanshanian orogeny, and propose a model in which tectonic movements and hydrothermal fluids modified the pre-existing magmatic sulfides. Given the high degree of overprinting, we suggest two possible scenarios: (1) sulfide disseminations that surround the massive magmatic ores are the result of deformation and hydrothermal alteration; and (2) both magmatic massive and disseminated sulfides were produced initially, in which case the scale and metasomatic remobilization would have been smaller, but still detectable.

Introduction

IN CHINA, the 825 Ma Jinchuan Ni-Cu-PGE deposit is the largest and best known (Li et al. 2005), with reserves of 500 million tons (Mt) at 1.2 wt% Ni and 0.7 wt% Cu; it is the third largest in the world, after Noril'sk and Sudbury (Naldrett, 2004 and references therein). Other economically significant Chinese Ni-Cu-PGE deposits include Huangshan (269 Ma; Zhou et al. 2004) and Kalatongke (285–298 Ma; Yan et al., 2003; Wang et al., 2004), both in Xinjiang Province, of Northwest China, and within the Altay and Tianshan orogens, respectively. The above deposits are hosted in mafic-ultramafic intrusions, probably related to mantle plume events (Zhou et al., 2002, 2004), but they do not appear to be associated with flood volcanism, although this may be due to levels of exposure beneath a cover of flood basalts that has since been eroded. By contrast in Southwest China, Ni-Cu-PGE and Fe-V-Ti oxide deposits are genetically and spatially associated with continental flood basalts of the Late Permian Emeishan large igneous province (ELIP; Fig. 1). One of these, the Baimazhai Ni-Cu-PGE deposit, constitutes the topic of this contribution.

In the ELIP apart from Baimazhai, other magmatic ore deposits include: the Ni-Cu-PGE sulfides at Yangliuping and Limahe (Song et al., 2003; Zhou et al., 2002); the PGE-dominated Lufangqing, Bading, and Dayanzi deposits (Yao et al., 2001); the

[1]Corresponding author; email: franco.pirajno@doir.wa.gov.au

Hongge Fe-V-Ti oxide ores (Zhong et al., 2002, 2003); and the V-Ti-Fe-PGE ores in the Pan-Xi district, e.g., Panzihua and Xinjie (Yao et al., 2001; Pang et al., 2005; Wang and Zhou, 2005a; Zhou et al., 2005). Exposures of the ELIP are present in northwestern Vietnam, where a komatiite-basalt complex hosts the Ban Phuc Ni-Cu-PGE deposit (Glotov et al., 2001). In addition, Keeweenawan-type deposits (native Cu in amygdaloidal basaltic lavas and associated sedimentary rocks; Brown, 1979) have been reported along the border area between Yunnan and Guizhou provinces (Zhu et al., 2003). About 35 km southeast of Baimazhai lies the Niulanchong Ni prospect, hosted by a gabbro sill associated with the Emeishan basaltic lavas (Fig. 2).

In this paper, we report some unusual textural features that characterize the magmatic Baimazhai Ni-Cu-PGE deposit. The host mafic and ultramafic rocks exhibit pervasive hydrothermal alteration which, we suggest, resulted in the modification of parts of the original magmatic sulfide ores. Ar-Ar age data support our model, as is explained below.

Geological Setting

The ELIP covers an area of at least 250,000 km^2 (Chung et al., 1998; Chung and Jahn, 1995; but according to Xiao et al., 2003 this is a conservative estimate) in Southwest China (Yunnan, Sichuan and Guizhou provinces), and in northwestern Vietnam (Fig. 1). The western boundary of the ELIP is the Ailao Shan Red River fault zone (ASRR), a major crustal structure separating the Yangtze craton from the Gandise and Yunnan fold belts (Fig. 1 and inset).

The ELIP consists of a succession of predominantly tholeiites, with minor picritic and rhyolitic lavas. In addition to flows, mafic-ultramafic layered complexes, dikes and sills, syenite, and other alkaline intrusions are part of the ELIP (Xu et al., 2001; Boven et al., 2002; Zhang Z. C. et al., 2004; Xiao et al., 2004a, 2004b). The maximum thickness of the lava flows is estimated at about 5400 m in the Pan-Xi rift (Binchuan region), decreasing to less than 500 m eastward from the rift (He et al., 2003; Xiao et al., 2003, 2004a, 2004b; Xu et al., 2004). In the Binchuan area, the volcanic stratigraphy (Xiao et al., 2003, 2004a, 2004b) consists of six units from amygdaloidal basalts (Unit 1 at the base), hyaloclastites, aphyric basalts (Unit 2), porphyritic and aphyric basalts, hyaloclastites (Units 3, 4, and 5) to trachytic lavas (Unit 6) at the top. This succession overlies limestones of the Middle Permian Maokou Formation, and is overlain by Triassic clastic sedimentary rocks of the Longtan Formation.

Xu et al. (2001) distinguished two main magma types that produced the lava flows, low-Ti (Ti/Y < 500; Mg# 44–67; εNd(t) 0.34–3.76), and high-Ti (Ti/Y > 500; Mg# 31–53; εNd(t) 1.17–0.43), with the latter further subdivided into three subtypes: HT1, HT2, and HT3. HT1 lavas are characterized by significantly high TiO_2 (3.65–4.7 wt%) and Nb/La (0.75–1.1), and low SiO_2 (45–51 wt%); HT2 lavas are geochemically similar to HT1 except that they are depleted in U and Th with respect to HT1; HT3 lavas have higher Mg# (0.51–0.61). Based on geochemistry, Xiao et al. (2003, 2004a, 2004b) distinguished two types of low-Ti magmas, LT1 and LT2. LT1 lavas exhibit higher Mg# (51–67) and ($^{87}Sr/^{86}Sr$)I ratios (0.706–0.707) than the LT2 lavas (Xiao et al., 2004a). The results of these studies indicate that the ELIP LT melts were derived from enriched mantle lithosphere, with a trend from shallower (LT1) to deeper lithospheric mantle (LT2). The HT magmas, on the other hand, apparently formed directly from a mantle plume.

SHRIMP zircon U-Pb dating of ELIP mafic and ultramafic intrusions yielded ages ranging from 259 ± 3 Ma to 262 ± 3 Ma (Zhou et al., 2002; Guo et al., 2004). Lo et al. (2002) reported high-precision $^{40}Ar/^{39}Ar$ dating between 251.2 ± 1 Ma and 252.1 ± 1.4 Ma, whereas Boven et al. (2002), also using the $^{40}Ar/^{39}Ar$ method, reported an age of 246 ± 4 Ma for the Panzhihua layered complex and an age of 254 ± 5 Ma from a pyroxenite. Additional $^{40}Ar/^{39}Ar$ ages (Ali et al., 2004) yielded younger ages, ranging from 147 to 42 Ma, which they attributed to thermal resetting due to tectonic events that affected the western Yangtze craton between the Jurassic–Cretaceous (Yanshanian orogeny) and the Eocene (Himalayan $^{40}Ar/^{39}Ar$ Alpine orogeny). This has important implications for the Baimazhai deposit, because one or both of these thermal events may have affected and modified the host rocks and sulfide ores at Baimazhai (and at the nearby Niulanchong Ni prospect as well).

The emplacement age of the ELIP indicates that it is coeval with the Siberian large igneous province (Siberian Traps; Sharma, 1997), which as already mentioned hosts the large Noril'sk Cu-Ni-PGE deposits. The contemporaneity of the Emeishan and Siberian events also led to proposals of possible Ni-Cu-PGE enriched superplume activity (Yakubchuk and Nikishin, 2004).

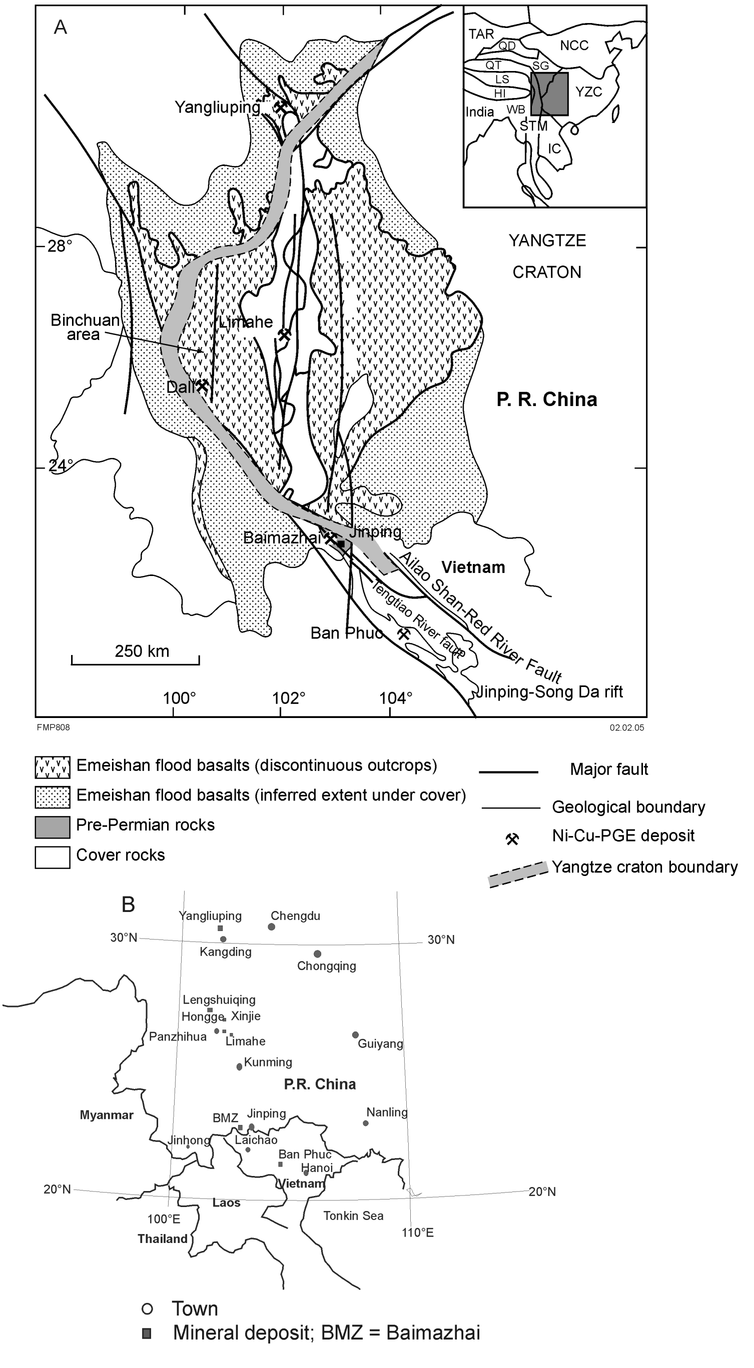

FIG. 1. A. Simplified geological map and inferred extent of the Emeishan large igneous province (ELIP) and distribution of selected Ni-Cu-PGE deposits. Inset shows position of the ELIP region and main tectonic units of China and adjacent countries (after Xu et al., 2001): Abbreviations: NCC = North China craton; YZC = Yangtze craton; QT = Qiangtang Block; LS = Lhasa Block; QD = Qaidam Block; TAR = Tarim Block; HI = Himalaya fold belt; WB = West Burma Block; STM = Shan-Thai-Malay Block, IC = Indochina Block. B. Distribution of known mineral deposits, main population centers, and international boundaries in southern Yunnan province and northern Vietnam.

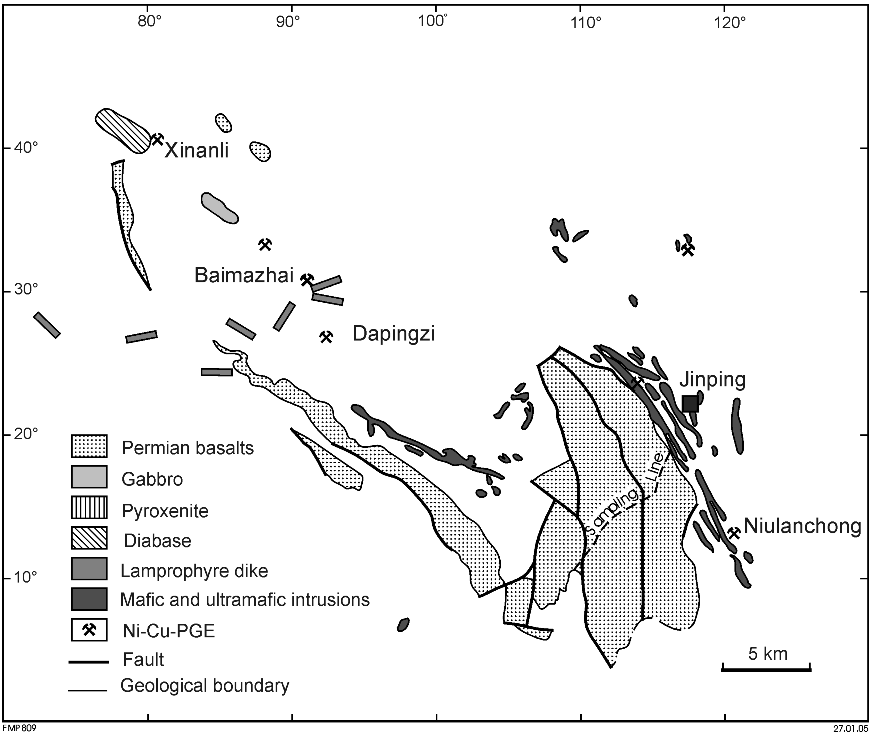

FIG. 2. Simplified geological map of the Jinping area, showing position of the Baimazhai and other Ni-Cu-PGE deposits.

Geology of the Deposit

The Baimazhai Ni-Cu deposit is located at N 22°51'15", E 102°59'33", near the town of Jinping, on the southwestern margin of the Yangtze craton, and within the Jinping-Song Da rift, in southeastern Yunnan Province (Figs. 1 and 2). The geology, geochemistry, and origin of the Baimazhai deposit have been reported by Tang et al. (1992), Wang et al. (2004), and Wang and Zhou (2005b). Other publications that deal with various aspects of the Baimazhai deposit include Song et al. (2003, 2005), Song and Zhu (2004), Zhang X. S. et al. (2004, 2005). This section summarizes the geology of the Baimazhai deposit, based on the works cited above, complemented with our own field observations.

The area around Jinping is underlain by Lower Ordovician clastic sedimentary rocks, Silurian and Devonian siltstone, shale, and limestone. These strata are intruded by a series of NW-trending mafic and ultramafic layered sill-like bodies extending along a strike of about 20 km. To the west of this mafic-ultramafic sill zone and separated by a NW-trending fault, is a thick (about 4.5 km) succession of flood basalts (Table 1). Syenite porphyry and lamprophyre dikes crosscut the sedimentary units, the volcanic rocks, and the sills. Elongate intrusions of biotite granite, quartz monzonite, and nepheline-acmite syenite lie to the east of the zone of sills. The age of the plutons in this area is not known, but similar rocks occurring elsewhere along the ASRR fault have isotopic ages ranging from 181 to 30 Ma (Hou et al., 2002, 2003; Wang et al., 2002; Hu et al., 2004; Guo et al., 2005).

The Baimazhai Ni-Cu ore deposit is hosted by three mafic-ultramafic intrusions (named No. 1, 2, and 3; Fig. 3) emplaced into Lower Ordovician sedimentary rocks of the Baimazhai Formation (locally also known as Xiangyang Formation; Table 1). The intrusions and the ore bodies are cut by lamprophyre dikes. The No. 2 and 3 intrusions contain massive sulfides, but only No. 3 has economically viable grades (Ni and Cu up to 3.5% and 2.3%, respectively; Wang and Zhou, 2005b). The deposit in the No. 3 intrusion has reserves of 50,000 tons of

TABLE 1. Volcanic Rock Stratigraphy in the Baimazhai Area[1]

Rock description	Thickness (m)
Massive, amygdaloidal basalts interbedded with volcaniclastic layers	162
Porphyritic basalt with intercalated purple tuffs	200
Massive, amygdaloidal basalt	329
Trachybasalts	309
Massive, amygdaloidal basalts, porphyritic basalts, and intercalated tuffs	677
Interbedded massive basalt, amygdaloidal basalt, and purple tuff	187
Massive basalt, amygdaloidal basalt	269
Amygdaloidal basalt	493
Massive basalt	117
Hyaloclastite basaltic lavas, amygdaloidal basalt, and trachybasalt	1498

[1]Uppermost rock units appear at the top of the table, and lowermost at the bottom.

Ni metal, with a total resource of about 100,000 tonnes of Ni metal (unpublished data obtained from the mine staff).

The No. 3 intrusion is banana-shaped, approximately 500 m long, 190 m wide, and up to 64 m thick (Tang et al., 1992; Wang and Zhou, 2005b), and consists of a mafic shell enclosing a core of ultramafic rocks, which host the massive sulfides (Fig. 4). From the margins to the core, rock types are: gabbro, pyroxenite, olivine-pyroxenite, and peridotite. These rock types, all show substantial to pervasive alteration to assemblages containing varying amounts of amphibole, chlorite, quartz, talc, and carbonate. The cross-cutting lamprophyre dikes were not affected by this hydrothermal alteration. Gabbro and pyroxenite have sharp contacts. Pyroxenite has fine-grained marginal or border facies, suggesting that it formed later.

Greyish green gabbro is from 2 to 55 m thick and forms the outer shell of the No. 3 intrusion. It is thinner at the base of the intrusion and thicker along the edges and tends to become richer in FeMg minerals towards the center. The gabbro is fine-grained with a hypidiomorphic-granular texture and is composed mainly of plagioclase, pyroxene, and brown hornblende, with accessory quartz, ilmenite, magnetite, and sulfides. Plagioclase is generally replaced by prehnite, penninite, and calcite and in most instances only the original outline of the crystals remained. Brown hornblende forms subhedral grains and is commonly replaced by tremolite-actinolite, and more rarely talc and penninite (Tang et al., 1992). The mineral assemblage of the least altered rock consists of plagioclase (about 40–60 vol%), clinopyroxene (up to 30 vol%), and tremolite (up to 50 vol% in places), which tends to replace the pyroxene. Ilmenite and apatite (3–5 vol%) are accessory minerals. Where present, alteration is pervasive and includes assemblages containing various proportions of epidote, carbonate, biotite, quartz, chlorite, tremolite-actinolite, and talc.

Greyish-green to brown pyroxenite is also fine-grained, from 2 to 9.5 m thick, and is situated between the gabbro and olivine-pyroxenite, but in the northern parts is in direct contact with peridotite. Locally, with increasing olivine content a transition zone to olivine-pyroxenite is present, but elsewhere the contacts are sharp. Pyroxenite is also strongly altered to chlorite (15–30 vol%), talc (up to 20 vol%), and tremolite (up to 85 vol%), and exhibits idiomorphic to hypidiomorphic granular texture. Other alteration phases include talc, serpentine, actinolite, and clinochlore. Although most or all primary rock-forming minerals have been completely altered, the original minerals can be recognized by crystal shapes. On this basis, this rock type is composed of short prismatic pyroxene crystals (0.2–1.2 mm), long prismatic brown hornblende (0.3–1.6 mm), some olivine, and accessory ilmenite, magnetite, chrome spinel, and sulfides (Tang et al., 1992).

Greenish olivine-pyroxenite is from 0.5 to 13 m thick and surrounds the peridotite unit, with sharp

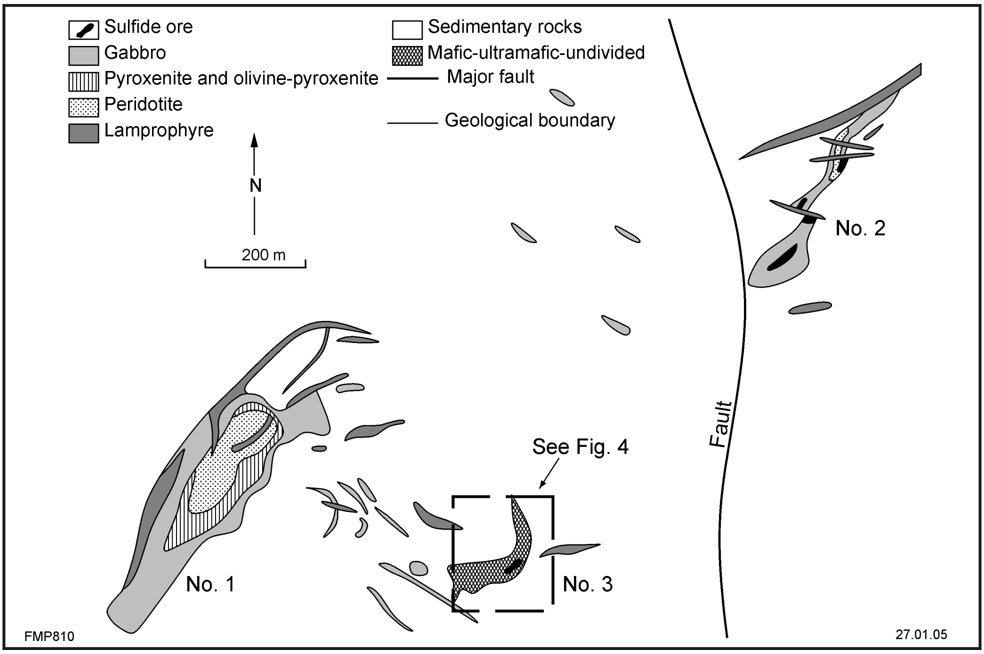

FIG. 3. Geological map of Baimazhai intrusions Nos. 1, 2, and 3 .

contacts near the surface and subsurface, but with transitional contacts at depth. All primary minerals are altered. This rock consists of talc (40–55 vol%), tremolite (20–40 vol%), serpentine olivine pseudomorphs (10–30 vol%), and lesser quantities of carbonate (dolomite), quartz, chlorite, mica phlogopite, sphene, and apatite. In the lower parts, this rock is entirely altered to talc-carbonate, and locally also contains secondary biotite.

Dark green peridotite is 9 m thick and lies at the core of the intrusion; it generally forms a ring around the sulfide ores. The peridotite has a hypidiomorphic granular texture or a cumulus-intercumulus texture where sulfides are present. Peridotite is strongly altered, but retains the original shape of its component crystals as pseudomorphs. Primary minerals include olivine, clino- and orthopyroxene and brown hornblende, with accessory ilmenite, magnetite, chrome spinel, and sulfides. Olivine pseudomorphs make up about 30 to 60 vol%. This olivine is present as euhedral crystals from 0.2 to 1 mm in size, and has been replaced entirely by antigorite, tremolite, and talc. Likewise, orthopyroxene is replaced by serpentine and talc, whereas clinopyroxene is replaced by tremolite, clinochlore, and penninite. Brown hornblende is replaced by tremolite and penninite. Other alteration minerals are carbonate, phlogopite, actinolite-tremolite, and biotite. An estimate of modal percentages are as follows: olivine and pyroxenes from 20 to 55 vol%, talc 20 to 40 vol%, and penninite 10 to 30 vol%.

Mineralization

The principal styles of mineralization are: disseminated, alteration-modified disseminated, net-textured, and massive ores (Figs. 4A and 4B). Tang et al. (1992) described the Baimazhai ore mineralogy in detail, and a summary of their work, integrated with additional data from the present study, is given below.

Disseminated ores are present in gabbro and pyroxenite and are generally distributed around the margins of the massive sulfide ore body, effectively forming a shell. Sulfides, 0.5 to 3.5 mm across, are unevenly disseminated between the silicate grains and have a volume percentage of between 6 and 12%. The ore minerals include pyrrhotite, pentlan-

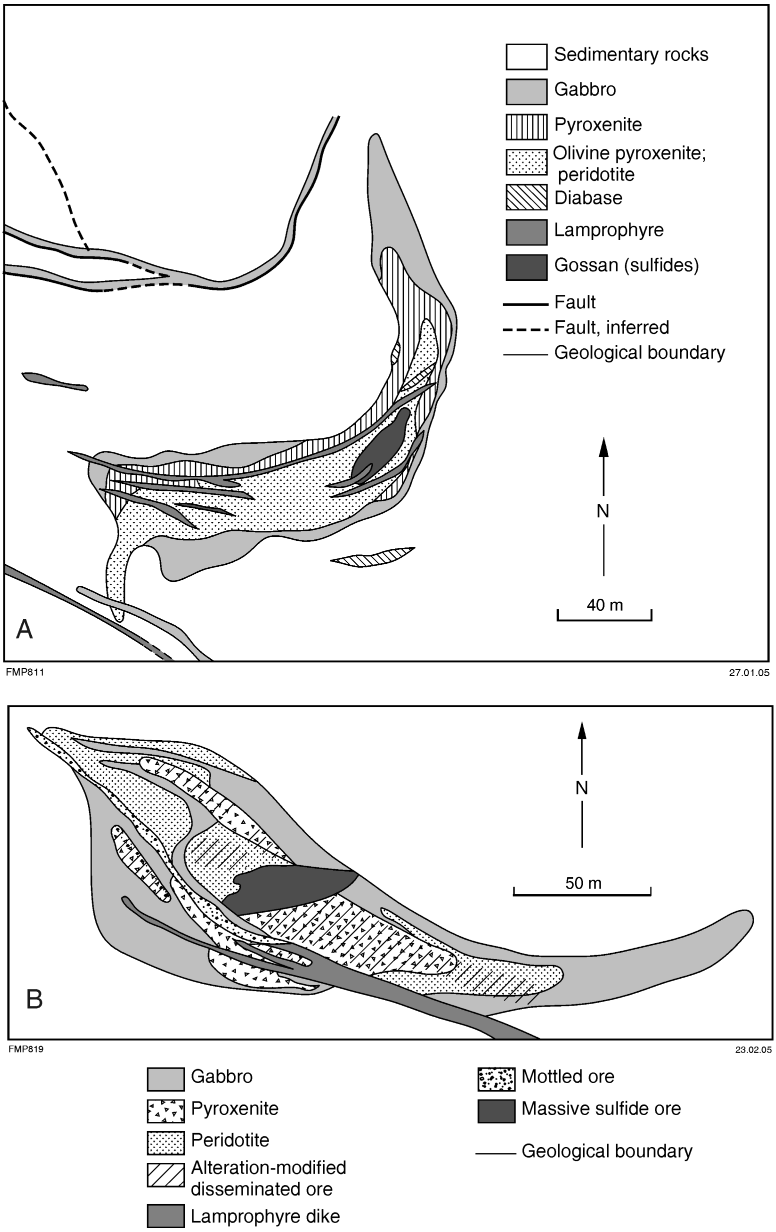

FIG. 4. Plan view of the geology of the No. 3 intrusion (A) and level No. 11 of the ore body (B).

dite, pyrite, marcasite, chalcopyrite, and violarite with trace amounts of magnetite, ilmenite, and chrome spinel. In gabbro host, the sulfides are finer-grained than in the pyroxenite host. The ratio of pyrrhotite:pentlandite:chalcopyrite is 53:2:1.

The distribution of *alteration-modified disseminated* ores is shown in Figure 4B. These form tabular bodies within the zones of disseminated sulfides. Here the ore mineral content is from 15 to 30 vol%, the sulfides have irregular or ovoid shapes (Figs. 5A

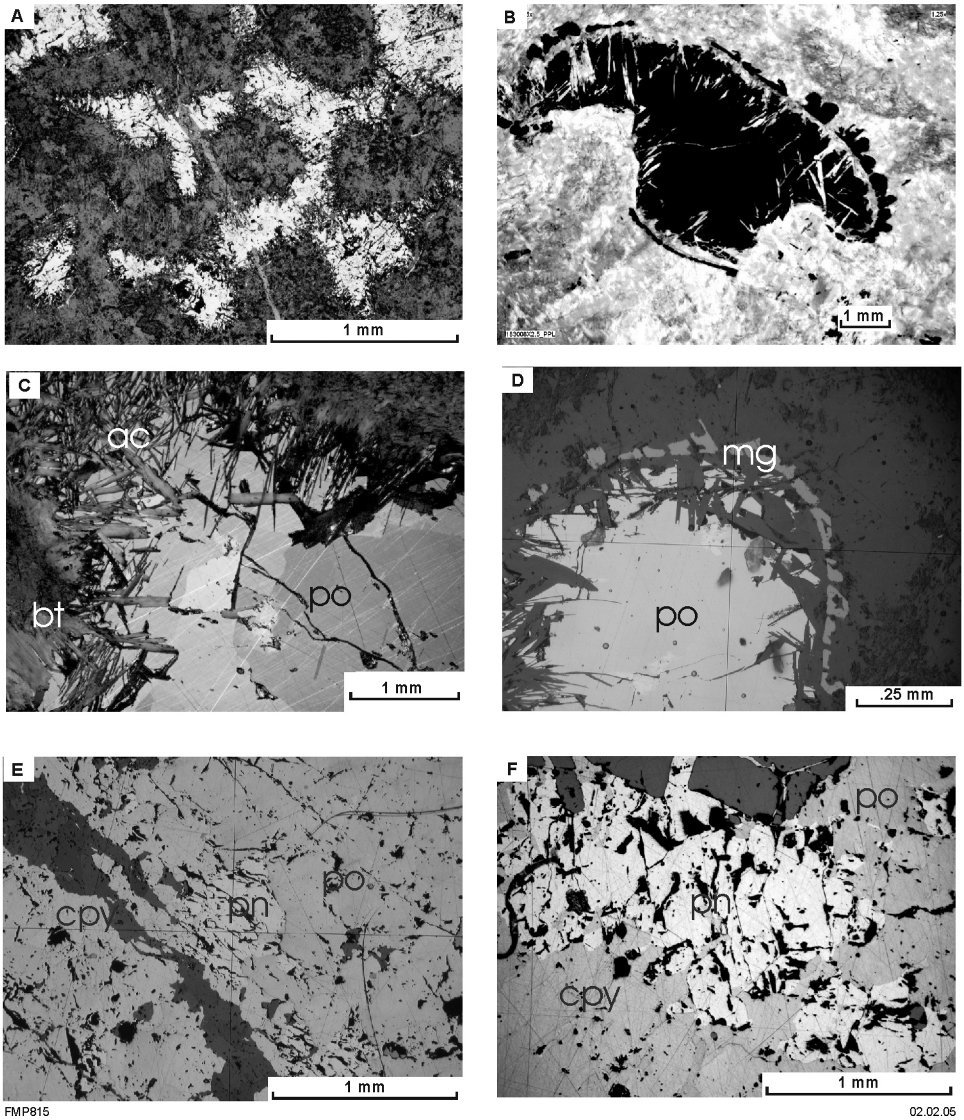

FIG. 5. Reflected light photomicrographs showing (A, B) alteration-modified disseminated pyrrhotite; the host matrix is pervasively altered to an assemblage that consists of actinolite, biotite, and chlorite; (D) the margins of pyrrhotite (po) are intergrown with biotite (bt) and actinolite (ac) and are commonly rimmed by a ring of magnetite (C). Reflected light photomicrographs (E) and (F) show the association of chalcopyrite (cpy), pyrrhotite (po), and pentlandite (pn) in the massive sulfide ore.

and 5B), and locally occur as abundant veinlets. Ore minerals comprise pyrrhotite, pentlandite, chalcopyrite, magnetite, chrome spinel, and ilmenite with trace amounts of galena, Ni-cobaltite, and parkerite ($Ni_3(Bi,Pb)_2S_2$. The ratio of pyrrhotite: pentlandite:chalcopyrite is 14:1.4:1. Sulfides in these ores characteristically fill microfractures of alteration minerals and are commonly associated with a brown biotite (possibly phlogopitic), actinolite-tremolite, and chlorite, which not only form the host groundmass, but also tend to be intergrown with the margins of the sulfide grains, imparting a peculiar barbed texture (Figs. 5A–5D).

Net-textured and massive sulfides form flat, tabular bodies in the center of the host rock and are locally transgressive across the igneous layers (Wang and Zhou, 2005a, 2005b) (Figs. 4A and 4B). The transgressive structure could be either an original feature that resulted from the emplacement of the sulfide liquid, or due to later tectonic deformation. The content of net-textured sulfides is from 15 to 30 vol%, whereas in the massive ore the sulfide content reaches 90 to 99 vol%. Both net-textured and massive ore minerals include pyrrhotite, pentlandite, chalcopyrite (Figs. 5E–5F), and magnetite with minor galena, parkerite, argentopentlandite, Ni-colbaltite, mackinawite, altaite, and electrum (Tang et al., 1992). Mackinawite is present in very small amounts, and is less than 0.05 mm in size. It occurs in flame form within chalcopyrite or at the contact between magnetite and chalcopyrite and penetrates into chalcopyrite. It is probably a product of exsolution, but in a few cases it also occurs within fine-grained pentlandite. Argentopentlandite $(Ag_{0.619–0.748}, Ni_{3.394–2.826}, Fe_{4.331–4.147}, Cu_{0.009})_{8.344–7.730}S_8$ is fine grained, less than 0.05 mm in size, and displays a light reddish brown reflection color, which is similar to that of bornite and djerfisherite but slightly brighter; it forms graphic intergrowths with fine-grained seriate-textured pentlandite and is replaced by late-stage chalcopyrite. Ni-cobaltite is euhedral, less than 0.05 mm across, and mainly occurs within pyrrhotite. Altaite occurs as small grains, 0.01 mm across, only within chalcopyrite. Electrum is found in fissures in pyrrhotite. Textural relationships indicate that pentlandite and pyrrhotite crystallized first, followed by Ni-cobaltite, chalcopyrite, argentopentlandite, and parkerite, whereas galena, mackinawite, altaite, and electrum formed in the latest stages. The ratio of pyrrhotite:pentlandite:chalcopyrite is 12:7:1. An unusual feature of the massive ores is the relatively high content of Ag and In (in argentopentlandite and electrum; Tang et al. 1992).

In addition to disseminated, alteration-modified disseminated, and massive ores, brecciated and "mottled" (local term for irregular patches of pyrrhotite and chalcopyrite aggregates) ores also occur. Breccias are present in sandstone and gabbro, where the component clasts are cemented by sulfides. Breccia ores contain the same sulfides as in the massive ores, but with a relatively higher content of chalcopyrite. The ore minerals include pyrrhotite, pentlandite, and chalcopyrite. The grains are about 0.1 to 0.3 mm across. The Cu content is generally higher than that in the massive ores. Some quartz and carbonate are present. The "mottled" ore is hosted by gabbro, with the sulfides forming pisolitic-like or droplet-like aggregates with grain size ranging from 5 to 15 mm.

Age Constraints for Baimazhai Mineralization

SHRIMP zircon U-Pb dating of the Baimazhai intrusion yielded an age of 258.5 ± 3.5 Ma (Wang et al., 2004). Other magmatic deposits that are related to the ELIP have ages of 263 ± 3 Ma and 262 ± 2 Ma (Panzhihua and Baima Fe-Ti-V, respectively) and 263 ± 3 Ma (Limahe Ni-Cu sulfide deposit) (Zhou et al. 2005; Fig. 1). All these deposits are coeval with the Emeishan flood basalts, with which the mafic-ultramafic rocks hosting the deposits are intimately associated.

The Baimazhai Ni-Cu sulfides and hydrothermally altered host rock are crosscut by unaltered lamprophyre dikes (Guan et al., 2003). Although the age of these dikes in the Jinping area is unknown, a belt of alkaline rocks, including lamprophyres and syenites, is present along the ASRR fault system, with ages ranging from 40 to 30 Ma (Wang et al., 2001; Hu et al., 2004; Guo et al., 2005). Post-Permian tectonothermal events in China (see Zhou et al., 2002 for an overview) are: the Indosinian orogeny (260–208 Ma), the Yanshanian orogeny (190–90 Ma), and the Himalayan orogeny (65–0 Ma). If we assume that the lamprophyre dikes at Baimazhai are of Himalayan age (40–30 Ma), then the hydrothermal event at Baimazhai is bracketed between the Indosinian and Yanshanian orogenies (260–90 Ma).

An attempt was made to constrain the age of mineralization by using the $^{40}Ar/^{39}Ar$ method on selected whole rocks (peridotite, pyroxenite, and gabbro). These age determinations were carried out by Guiling Minerals and Resources Institute (Guiling City). A summary of the results is presented in Table 2 (details of the results and step-heating data are available on request from the corresponding author). As shown in Table 2, calculated ages range from 170.02 ± 3.4 to 160.48 ± 3.32 Ma (Middle Jurassic). These ages are in marked contrast with the Permo-Triassic boundary age of the ELIP. The 160–170 Ma age range obtained in this work is

TABLE 2. $^{39}Ar/^{40}Ar$ Whole-Rock Dating Results

Sample no.	Rock	Type[1]	Age, Ma
BMZ 01	gabbro	Tp	167.96 ± 1.8
		Tiso	170.02 ± 3.4
		Tf	167.97 ± 3
BMZ 10	pyroxenite	Tp	164.17 ± 2.5
		Tiso	160.48 ± 3.32
		Tf	164.16 ± 3.8
BMZ 11	peridotite	Tp	166.78 ± 1.8
		Tiso	164.51 ± 3.29
		Tf	166.97 ± 3

[1]Abbreviations: Tp = age calculated on turning point of heating curve; Tf = age from melting sample; Tiso = isochron time. Details are discussed in the text.

consistent with the $^{40}Ar/^{39}Ar$ age clusters (±175 Ma) reported by Ali et al. (2004) and ascribed to resetting due to a 177–135 Ma collision event (Ali et al., 2004; Hou et al., 2002), that brought together the Lhasa Block and the Qiantang-Indochina Block (see Inset of Fig. 1). This tectonic event, which was accompanied by the intrusion of granodiorite plutons (Wang et al., 2002), falls within the age range of the Yanshanian orogeny (190–90 Ma).

A Model for the Origin of Hydrothermally Modified Magmatic Sulfides

A generally accepted model of ore genesis for mafic-ultramafic hosted massive and disseminated Ni-Cu sulfide ores calls on immiscibilty between a silicate melt and a sulfide liquid. Magmatic segregations of the Ni-Cu sulfides was probably facilitated by introduction of crustal sulfur into an originally S-undersaturated silicate melt (e.g., Keays 1995; Naldrett 1997). The Baimazhai ores had an orthomagmatic origin and are considered to have been the result of multiple melt injections along the same conduit (Tang et al., 1992). Wang et al. (2004) suggested that the Baimazhai sulfide deposit was formed by the emplacement of an olivine- and sulfide-rich crystal mush. Due to immiscibility, the sulfide liquid was subsequently concentrated in the center of the intrusion (Zhang et al., 2004; Wang and Zhou, 2005b). The latter authors reported εNd values ranging from –3.3 to –8.4 for the Baimazhai rocks, and suggested that these low εNd values are consistent with crustal contamination and subsequent S oversaturation, which induced precipitation of sulfides. Wang and Zhou (2005b) further suggested that the Baimazhai intrusion was derived from a staging magma chamber lodged in the crust.

At Baimazhai, there is convincing field, petrographic, and textural evidence of hydrothermal alteration of the intrusive rocks, during which the silicate minerals were pervasively replaced by hydrous phases (Fig. 6). Evidence of hydrothermal activity has been reported from other areas within the ELIP. For example, Li et al. (2005) discussed the epigenetic-hydrothermal features of Keewenawan type Cu mineralization in the basaltic lavas, mentioned earlier (Zhu et al., 2003). Dating of hydrothermal minerals such as laumontite, actinolite, and heulandite in the Cu-bearing basalts by the $^{40}Ar/^{39}Ar$ method yielded ages ranging from 238 to 134 Ma (Zhu et al., 2004). Li et al. (2005) commented that these ages are from 30 to 120 m.y. younger than the Emeishan basalts, and concluded that the Cu mineralization was later than the ELIP magmatic event and of hydrothermal origin.

The hydrothermal fluids may not have modified the entire body of massive sulfides, but it is possible that tectonic movements affected the mafic-ultramafic margins, forming zones of disrupted or brecciated sulfides. This would have facilitated the introduction of hydrothermal fluids resulting in disseminated and interstitial sulfide ores. The "alteration-modified" sulfides (Fig. 5) are interpreted as an example of this tectonic and hydrothermal activity. The process is also indicated by the presence of sulfide phases, other than the normal pyrrhotite-pentlandite-chalcopyrite assemblage, in which metal redistribution of certain trace elements such as Bi and Pb occurred to precipitate exotic sulfides (e.g., parkerite). Post-crystallization alteration of primary Ni-Cu sulfides results in the formation of Cu-rich ores, accompanied by mineral phases such as Pt- and Pd-rich arsenides, tellurides and Bi-bearing minerals (Watkinson and Melling, 1992; Farrow and Watkinson, 1999). These minerals are also associated with hydrous silicates (e.g., chlorite and sericite) and, importantly, with enrichment in Au and Ag, as in fact observed at Baimazhai. Therefore, these modified ores tend to be enriched in Cu, Au, and Pd (Table 3).

The model that we envisage for Baimazhai is schematically illustrated in Figure 7. In this model,

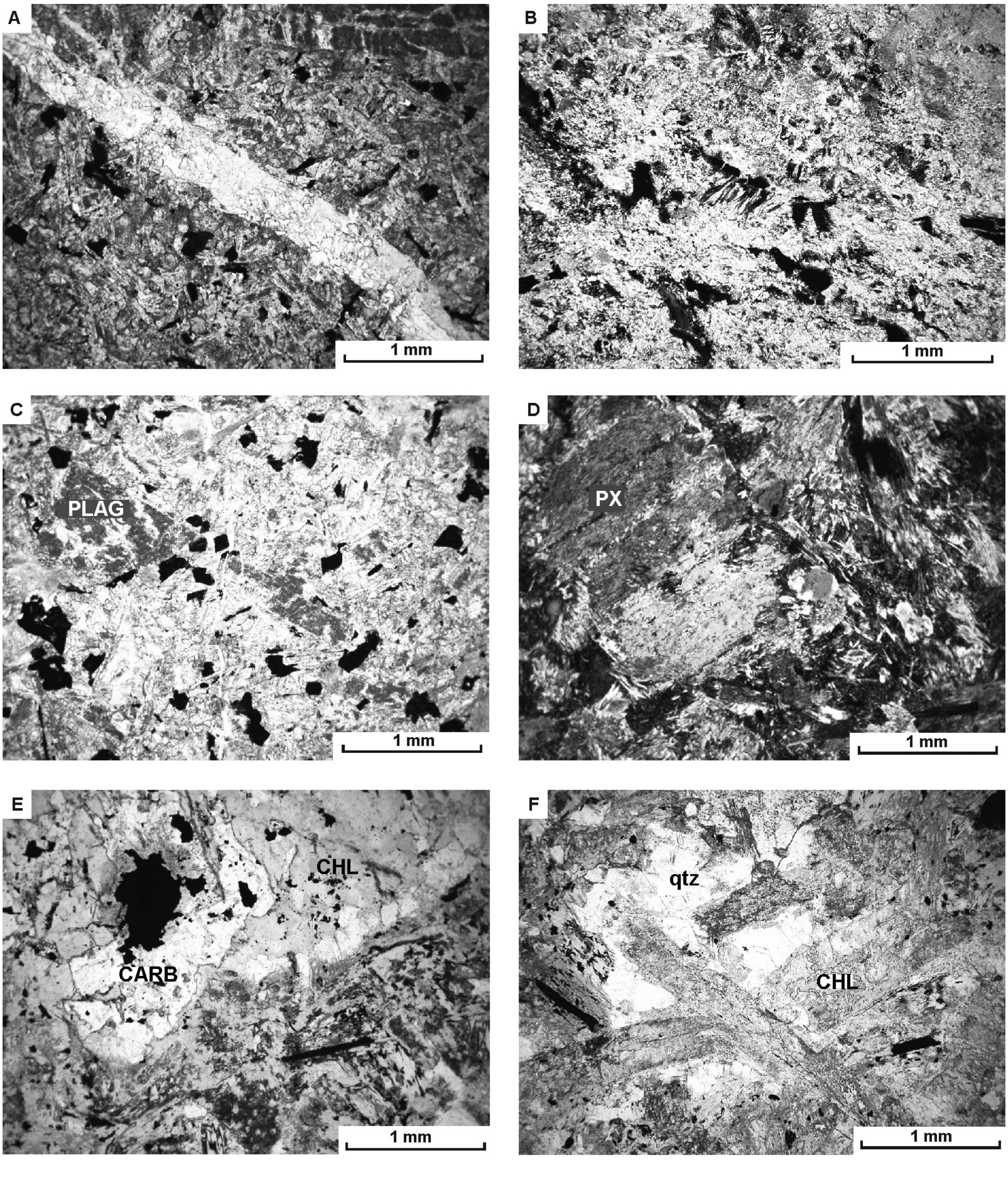

FIG. 6. Photomicrographs showing features of pervasive hydrothermal alteration of host rocks at Baimazhai and surrounding areas. A. Basaltic rock from the nearby Niewleuchang Ni prospect altered to a chlorite-carbonate-epidote assemblage, both in matrix and as cross-cutting veinlets. Opaques are ilmenites altered to titanite; here the basaltic texture is still recognizable; plane-polarized light. B. Pervasive talc-carbonate alteration of ultramafic rock; cross polars. C. Unidentified intrusive rock (possibly gabbro) altered to chlorite, carbonate, and quartz; the shape of a feldspar lath (PLAG) is still recognizable, plane-polarized light. D. Actinolite, chlorite, and biotite alteration of pyroxenite hosting alteration-modified sulfides; relic pyroxene crystal (PX) is still recognizable. E. Carbonate (CARB) and chlorite (CHL) pervasive alteration of fine-grained gabbro; black is sulfide. F. Quartz and chlorite alteration of gabbroic rock; feldspar laths are still recognizable.

TABLE 3. Ore Element Analyses of Baimazhai Sulfides

Ore type	Ni, wt%	Cu, wt%	Co, wt%	S, wt%	Au, ppb	Ag, ppm	Pt, ppb	Pd, ppb	As, ppm	Bi, ppm
Massive sulfide ore (3)[1]	3.76	1.69	0.197	35.03	103	9.8	360	640	40	50
Breccia ore (2)	2.77	1.25	0.129	25.75	1140	10	400	400	50	40
Alteration-modified ore (4)	0.93	0.87	0.054	8.16	230	4.8	100	150	20	21
Disseminated ore (in peridotite) (4)	0.63	0.68	0.039	5.48	80	4.8	110	150	30	17
Disseminated ore (in pyroxenite) (4)	0.72	1.47	0.045	6.99	170	3.2	110	180	30	8
Mottled ore (in pyroxenite) (4)	0.57	0.46	0.035	5.43	280	3.8	50	50	50	3

[1]Numbers in parentheses indicate the number of samples analyzed.

we envisage two possible cases: (1) a massive sulfide body (Fig. 7A; Case 1) was deformed and its margins, which became disrupted and brecciated, formed a shell of disseminated sulfides around the massive ores (Fig. 7B; Case 1). This shell or envelope allowed the access of hydrothermal fluids, which texturally and perhaps compositionally modified the sulfides and the host rock (Figs. 7C and 7D; Case 1). (2) Alternatively, a magmatic massive sulfide body was originally associated with a zone of magmatic disseminated sulfides (Fig. 7A; Case 2). Upon deformation of the massive-disseminated sulfide system, hydrothermal fluids penetrated the most permeable zones represented by the disseminated sulfides (Figs. 7B and 7C; Case 2). In both cases, the contact between sulfides and wall rock is a zone of highest geochemical gradient as well as a favorable structural locale, and the fluids are expected to be focused within this zone.

Hydrothermal remobilization at Baimazhai was probably linked to post-magmatic regional tectonothermal events in the region. These events produced hydrothermal fluids that were focused into suitable structures, and the same fluids also modified existing mafic-ultramafic sulfide systems. No detailed structural data are available from the Baimazhai region, but limited field structural observations show that mylonites are present in the ASRR fault zone, and an overturned anticline affects the sedimentary rocks intruded by the Baimazhai plutons. Wang and Zhou (2005b) suggested that the Baimazhai magma was tectonically emplaced into Ordovician sedimentary rocks in a convergent-margin setting, at the boundary between the South China Block and the Indosinian Block. Moreover, quartz veins cut through the sulfide ores (Wang C.Y., pers. commun., 2005), further confirming the activity of hydrothermal fluids.

The Emeishan flood basalts were erupted at about 250 Ma, marking the impingement of a mantle plume beneath the western margin of the Yangtze craton (Xiao et al., 2003). The closure of the Paleotethys ocean and collision between the Indo-China Block and the Yangtze craton took place in Mid-Triassic time, forming the major ASRR fault zone and leading to the final amalgamation of the Indo-China terranes with the Yangtze craton and the South China Block. The ASRR and adjacent sutures were reactivated during the 55–50 Ma collision of the Indian plate with Eurasia. This reactivation of the ASRR is estimated at about 300 km of left-lateral strike slip movement (Tapponier et al., 1990).

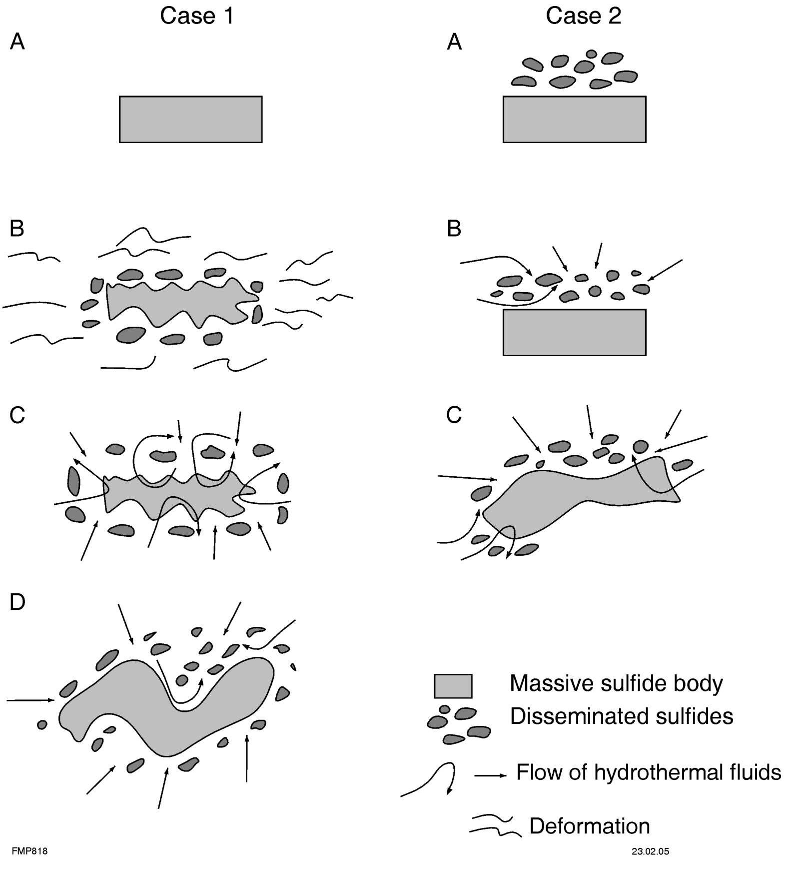

FIG. 7. Ore genesis model. *Case 1*, a magmatic massive sulfide zone (A), is subjected to deformation, resulting in the disruption of the sulfide zone along its margins, forming an envelope of disseminated sulfides (B). This is followed by an influx of hydrothermal fluids (C), which texturally and compositionally(?) modify the envelope of sulfide disseminations (D). *Case 2*, the original magmatic ore zone, consists of massive and disseminated sulfides (A); during deformation hydrothermal fluids penetrate the easily accessible zone of disseminated sulfides (B), resulting in the observed textural modifications (C). Further details are provided in the text.

Movement along the ASRR was coincident with regional prograde metamorphism up to amphibolite facies, and predominantly alkaline magmatic activity during the Eocene–Oligocene (Qian, 1999; Guo et al., 2005).

As previously mentioned, Ali et al. (2004) used ^{40}Ar-^{39}Ar dating to chronologically define the post-Permian tectonothermal events in the Indo-China–western Yangtze region, affected by the Emeishan flood volcanism. These events cluster at ca. 175, 142, 98, and 42 Ma, which Ali et al. ascribed to strike-slip and collisional tectonic movements along the complex major sutures that separate the Indian block in the west from the Indo-China and the South China blocks to the east and the Songpan-Garze Basin to the northwest. We suggest that the ~170 Ma ^{40}Ar-^{39}Ar ages reported in this study most likely indicate a thermal resetting in the Middle Jurassic. Ali et al. (2004) attributed their ~175 Ma ages to a resetting caused by strike-slip movements along the Qinling-Dabie suture that separates the North China and South China blocks. It is also possible that hydrothermal modification of the Baimazhai sulfide system was the result of tectonic motion along the ASRR fault zone during the Himalayan orogeny, which also resulted in the emplacement of alkaline igneous rocks (lamprophyre and syenites) in the zone. The age of this magmatism in southeastern Tibet and Yunnan Province is constrained by the ^{40}Ar-^{39}Ar age date between 32 and 34 Ma (Guo et al., 2005). If this is the correct interpretation, then the whole-rock ^{40}Ar-^{39}Ar ages for the Baimazhai deposit could represent a "mixed" resetting between the 260 Ma time of the Emeishan flood basalts and the Himalayan tectonothermal events (65–0 Ma).

Conclusions

The mafic-ultramafic rocks that host the Baimazhai sulfides exhibit pervasive hydrothermal alteration. Thin section and ore microscopy studies of disseminated sulfide ores suggest that the latter were modified during post-magmatic sulfide remobilization or relocation. This is especially evident in the altered-disseminated ores (Fig. 5). Remobilization of sulfide ores is not uncommon and is usually linked with regional high-grade metamorphism (Marshall et al., 2000). The specific effects of hydrothermal alteration on sulfide ores are less known, but as pointed out by Tomkins et al. (2004), dehydration reactions during prograde metamorphism produce hydrothermal fluids that have the capacity to dissolve sulfides and remobilize their constituents, resulting in both textural and mineralogical changes. Presence of the alteration minerals biotite and chlorite is indicative of halogen volatile activity (e.g., Cl). The halogen activity is considered by several authors to result in the remobilization of PGE-bearing and other base metal phases (McCallum et al., 1976; McCandless and Ruiz, 1991; Boudreau and McCallum, 1992). The occurrence of biotite, chlorite, and amphibole intergrown with sulfides is additional evidence of volatile activity (Farrow and Watkinson, 1999).

The resetting of $^{40}Ar/^{39}Ar$ ages, hydrothermal alteration, and associated modification of disseminated sulfide ores suggest that the Baimazhai Ni-Cu-PGE sulfide deposit interacted with hydrothermal fluids that were most likely generated by a tectonothermal event that affected the region in the Jurassic (Hou et al., 2002; Wang et al., 2002). The precise nature of the interaction between the hydrothermal fluids and magmatic sulfides is not known, and more work is needed.

Perhaps Cu-rich nickeliferous ores in mafic-ultramafic systems can be explained using the hydrothermal model, considering the possibility that the Cu (and Pd) enrichment may have been related to post-magmatic modification of sulfide ores by interaction with late hydrothermal fluids. Our study is of a preliminary nature; however, we plan to further develop this work employing trace element and isotope geochemistry. At the same time we invite other geoscientists working on mafic-ultramafic mineralized systems to evaluate and test our model.

Acknowledgments

This paper is based on the field and laboratory studies during the period from 2001 to 2004, with financial support from an SEG Student Grant and the Yunnan Provincial Government (Project No. 2002GH11). The authors wish to acknowledge generous support by the staff of the Baimazhai nickel mine. Valuable contributions are acknowledged from Prof. Qin Dexian of Kunming University of Science and Technology, Prof. Ren Zhiji of Yunnan Nonferrous Metals Geological Bureau, and Zoran Seat of the University of Western Australia. Mr. Chen Minyang performed the $^{39}Ar/^{40}Ar$ analyses at the Guiling Minerals and Resources Institute. Michael Prause and Susanne Dowsett (Geological Survey of Western Australia) drafted the figures. Christina Yan Wang and Prof. Mei-Fu Zhou (both of Hong Kong University) are thanked for their comments and for providing critical additional knowledge of the Baimazhai deposit. Franco Pirajno publishes with the permission of the Director of the Geological Survey of Western Australia.

REFERENCES

Ali, J. R., Lo, C. H., Thompson, G. M., and Song, X. Y. 2004, Emeishan basalt Ar-Ar overprint ages define several tectonic events that affected the western Yangtze platform in the Mesozoic and Cenozoic: Journal of Asian Earth Sciences, v. 23, p. 163–178.

Boven, A., Pasteels, P., Punzalan, L. E., Liu, J., Luo, X., Zhang, W., Guo, Z., and Hertogen, J., 2002, $^{39}Ar/^{40}Ar$ geochronological constraints on the age and evolution of the Permo-Triassic Emeishan volcanic province, southwest China: Journal of Asian Earth Sciences, v. 20, p. 157–175.

Boudreau, A. E., and McCallum, I. S., 1992, Concentration of platinum-group elements by magmatic fluids in layered intrusions: Economic Geology, v. 87, p. 1830–1848.

Brown, A. C., 1979, Stratiform copper deposits: Evidence for their post-sedimentary origin: Mineral Science and Engineering, v. 10, p. 152–170.

Chung, S. L., and Jahn, B. M., 1995, Plume-lithosphere interaction in the generation of the Emeishan flood basalts as the Permian-Triassic boundary: Geology, v. 23, p. 889–892.

Chung, S. L., Jahn, B. M., Wu, G. Y., Lo, C. H., and Bolin, C., 1998, The Emeishan flood basalts in SW China: A mantle plume initiation model and its connection with continental breakup and mass extinction at the Permian-Triassic boundary: American Geophysical Union, Geodynamic Series, v. 27, p. 47–58.

Farrow, C. E. G., and Watkinson, D. H. 1999, An evaluation of the roel of fluids in NI-Cu-PGE–bearing mafic ultramafic systems: Geological Association of Canada, Short Course Notes, v. 13, p. 31–67.

Glotov, A. I., Ployakov, G. V., Hoa, T. T., Balykin, P. A., Akimtsev, V. A., Krivenko, A. P., Tolstykh, N. D., Phuong, N. T., Thanh, H. H., Hung, T. Q., and Petrova, T. E., 2001, The Ban-Phuc Ni-Cu-PGE deposit related to the Phanerozoic komatiite-basalt association in the Song Da rift, northwestern Vietnam: The Canadian Mineralogist, v. 39, p. 573–589.

Guan, T., Huang, Z. L., and Xie, L. H., 2003, Geochemical characteristics of mantle source region of lamprophyres in Baimazhai nickel deposit, Yunnan province: Geochimica et Cosmochimica Acta (suppl.), v. 67, p. 127.

Guo, F., Fan, W. M., Wang, Y. J., and Li, C. W., 2004, When did the Emeishan mantle plume activity start? Geochronological and geochemical evidence from ultramafic-mafic dikes in southwestern China: International Geology Review, v. 46, p. 226–234.

Guo, Z. F., Hartogen, J., Liu, J. Q., Pasteels, P., Boven, A., Punzalan, L., He, H. Y., Luo, X. J., and Zhang, W. H., 2005, Potassic magmatism in Western Sichuan and Yunnan Provinces, SE Tibet, China: Petrological and geochemical constraints on petrogenesis: Journal of Petrology, v. 46, p. 33–78.

He, B., Xu, Y. G., Chung, S. L., Xiao, L., and Wang, Y., 2003, Sedimentary evidence for a rapid, kilometer-scale crustal doming prior to the eruption of the Emeishan flood basalts: Earth and Planetary Science Letters, v. 213, p. 391–405.

Hou, Z. Q., Chen, W., and Lu, J. R., 2002, Collision event during 177–135 Ma on the eastern margin of the Qinghai-Tibet plateau: Evidence from $^{40}Ar/^{39}Ar$ dating for basalts on the western margin of the Yangtze platform: Acta Geologica Sinica, v. 76, p. 194–204.

Hou, Z. Q., Ma, H. W., Zaw, K., Zhang, Y. Q., Wang, M. J., Wang, Z., Pan, G. T., and Tang, R. L., 2003, Himalayan Yulong porphyry copper belt: Product of large scale-scale strike-slip faulting in eastern Tibet: Economic Geology, v. 98, p. 125–145.

Hu, R. Z., Burnard, P. G., Bi, X. W., Zhou, M. F., Pen, J. T., Su, W. C., and Wu, K. X., 2004, Helium and argon isotope geochemistry of alkaline intrusion-associated gold and copper deposits along the Red River–Jinshajiang fault belt, SW China: Chemical Geology, v. 203, p. 305–317.

Keays, R. R., 1995, The role of komatiitic and picritic magmatism and S-saturation in the formation of ore deposits: Lithos, v. 34, p. 1–18.

Li, H. M., Mao, J. W., Chen, Y. C., Wang, D. H., Zhang, C. Q., and Xu, H., 2005, Epigenetic hydrothermal features of the Emeishan basalt copper mineralization in NE Yunnan, SW China. Mineral Deposits Research: Meeting the global challenge, *in* Mao, J. W., and Bierlein, F., eds., Proceedings of the 8th Biennial SGA Meeting, Beijing, v. 1, p. 149–152.

Li, X. H., Su, L., Chung, S.-L., Li, Z. X., Liu, Y., Song, B., and Liu, D. Y. 2005, Formation of the Jinchuan ultramafic intrusion and the world's third largest Ni-Cu sulfide deposit: Associated with the ~825 Ma South China mantle plume?: Geochemistry, Geophysics, Geosystems, v. 6 [doi: 10.1029/2005GC001006].

Lo, C. H., Chung, S. L., Lee, T. Y., and Wu, G. Y., 2002, Age of the Emeishan flood magmatism and relations to Permian–Triassic boundary events: Earth and Planetary Science Letters, v. 198, p. 449–458.

Marshall, B., Vokes, F. M., and Larocque, A. C. L., 2000, Regional metamorphic remobilization: Upgrading and formation of ore deposits: Reviews in Economic Geology, v. 11, p. 19–38.

McCallum, M. E., Loucks, R. R., Carlson, R. R., Cooley, E. F., and Doerge, T. A., 1976, Platinum metals associated with hydrothermal copper ores of the New Rambler mine, Medicine Bow Mountains, Wyoming: Economic Geology, v. 71, p. 1429–1450.

McCandless, T. E., and Ruiz, J., 1991, Osmium isotopes and crustal sources for platinum-group mineralization in the Bushveld Complex, South Africa: Geology, v. 19, p. 1225–1228.

Naldrett, A. J., 1997, Key factors in the genesis of Noril'sk, Sudbury, Jinchuan, Voisey's Bay, and other world class Ni-Cu-PGE deposits: Implications for exploration: Australian Journal of Earth Sciences, v. 44, p. 283–316.

Naldrett, A. J., 2004, Magmatic sulfide deposits—geology, geochemistry and exploration: Berlin, Germany, Springer-Verlag, 727 p.

Qian, X. G., 1999, A preliminary discussion about the petrology and genesis of Cenozoic volcanic rocks in Janchaun-Madeng and Heqing-Dianan areas, west Yunnan: Yunnan Geology, v. 18, p. 413–424 (in Chinese with English abstract).

Pang, K. N., Zhou, M. F., and Ma, Y. X., 2005, Fe-Ti-V oxide mineralization in the Permian Panzhihua gabbro, Emeishan large igneous province, SW China, *in* Mao, J. W., and Bierlein, F. P., eds., Mineral deposit research: Meeting the global challenge, v. 1: Proceedings of the 8th Biennial SGA Meeting, Beijing, China, p. 453–456.

Sharma, M., 1997, Siberian traps. American Geophysical Union Monographs, v. 100, p. 273–296.

Song, X. Y., Zhong, H., Tao, Y., and Zhou, M. F., 2005, Magmatic sulfide deposits in the Permian Emeishan large igneous province, SW China, *in* Mao, J. W., and Bierlein, F. P., eds., Mineral deposit research: Meeting the global challenge, v. 1: Proceedings of the 8th Biennial SGA Meeting, Beijing China, p. 465–467.

Song, L. J., and Zhu, J. Y., 2004, The model of geophysical metallogenic prognosis of the Baimazhai nickel deposit of Jinping County: Progress in Geophysics, v. 19, no. 1, p. 186–190 (in Chinese with English abstract).

Song, X. Y., Zhou, M. F., Cao, Z. M., Sun, M., and Wang, Y. L., 2003, Ni-Cu-PGE magmatic sulfide deposits in the Yangliuping area, Permian Emeishan igneous province, SW China: Mineralium Deposita, v. 38, p. 831–843.

Tang, Z. L., Ren, D. J., Xue, Z. R., and Mu, Y. K., 1992, Nickel deposits of China, *in* Mineral deposits of China, v. 2: Beijing, China, Geological Publishing House, p. 59–99.

Tapponier, P., Lacassin, R., Leloup, P. H., Scharer, U., Zhong, D. L., Wsu, H. W., Liu, X. H., Ji, S. C., Zhang, L. S., and Zhong, J. Y., 1990, The Ailao Shan/Red River metamorphic belt: Tertiary left-lateral shear between Indochina and South China: Nature, v. 343, p. 431–437.

Tomkins, A. G., Pattison, D. R. M., and Zaleski, E., 2004, The Hemlo gold deposit, Ontario: An example of melting and mobilization of a precious metal-sulfosalt assemblage during amphibolite-facies metamorphism and deformation: Economic Geology, v. 90, p. 1063–1084.

Wang, C. Y., and Zhou, M. F., 2005a, Mineral chemistry of Fe-Ti oxides from the Xinjie PGE-bearing layered mafic-ultramafic intrusion in Sichuan, SW China, *in* Mao, J. W., and Bierlein, F. P., eds., Mineral deposit research: Meeting the global challenge, v. 1: Proceedings of the 8th Biennial SGA Meeting, Beijing China, p. 481–485.

Wang, C. Y., and Zhou, M. F., 2005b, Origin of the Permian Baimazhai Ni-Cu-PGE sulfide deposit, Jinping, Southern Yunnan Province, SW China [abs.], *in* 10th Platinum International Symposium, Oulu, Finland, extended abstacts, part 5, p. 606–609.

Wang, C. Y., Zhou, M. F., and Keays, R. R., 2004, Origin of the Permian Baimazhai Ni-Cu-PGE sulfide deposit, Jinping, southern Yunnan Province, SW China [abs.]. *in* Proceedings IGCP 479, Hong Kong, abstracts, p. 76–78.

Wang, J. H., Qi, L., Yin, A., and Xie, G. H., 2001, Emplacement age and PGE geochemistry of lamprophyres in the Laowangzhai gold deposit, Yunnan, SW China: Science in China (Series D), v. 44, p. 146–154.

Wang, X. F., Metcalfe, I., Jain, P., He, L. Q., and Wang, C. S., 2000, The Jinshajiang-Ailaoshan suture zone, China: Tectonostratigraphy, age, and evolution: Journal of Asian Earth Sciences, v. 18, p. 675–690.

Wang, Y. J., Fan, W. M., Guo, F., Li, H. M., and Liang, X. Q., 2002, U-Pb dating of early Mesozoic granodioritic intrusions in southeastern Hunan Province, South China and its petrogenetic implications: Science in China (Series D), v. 45, p. 280–288.

Wang, Y. W., Wang, J. B., Wang, L. J., Wang, Y., and Tu, C. N., 2004, REE characteristics of the Kalatongke Cu-Ni deposit, Xinjiang, China: Acta Geologica Sinica, v. 78, p. 396–403.

Watkinson, D. H., and Melling, D. R., 1992, Hydrothermal origin of platinum-group mineralization in low-temperature copper sulfide-rich assemblages, Salt Chuk intrusion, Alaska: Economic Geology, v. 87, p. 175–184.

Xiao, L., Xu, Y. G., Chung, S. L., He, B., and Mei, H., 2003, Chemostratigraphic correlation of upper Permian lavas from Yunnan Province, China: Extent of the Emeishan Large Igneous Province: International Geology Review, v. 45, p. 754–766.

Xiao, L., Xu, Y. G., Mei, H. J., Zheng, Y. F., He, B., and Pirajno, F., 2004a, Distinct mantle sources of low-Ti and high Ti basalts from the western Emeishan large igneous province, SW China: Implications for plume-lithosphere interaction. Earth and Planetary Science Letters, v. 228, p. 525–546.

Xiao, L., Xu, Y. G., Xu, J. F., He, B., and Pirajno, F., 2004b, Chemostratigraphy of flood basalts in the Garze-Litang region and Zongza Block: Implications for western extension of the Emeishan Large Igneous Province, SW China: Acta Geologica Sinica, v. 78, p. 61–67.

Xu, Y. G., He, B., Chung, S. L., Jahn, B. M., and Wu, G. Y., 2001, Petrologic and geochemical constraints on the petrogenesis of Permian–Triassic Emeishan flood basalts in southwestern China: Lithos, v. 58, p. 145–168.

Xu, Y. G., He, B., Chung, S. L., Menzies, M. A., and Frey, F. A., 2004, Geologic, geochemical, and geophysical consequence of plume involvement in the Emeishan flood-basalt province: Geology, v. 32, p. 917–920.

Yakubchuk, A., Nikishin, A., 2004, Noril'sk-Talnakh Cu-Ni-PGE deposits: A revised tectonic model: Mineralium Deposita, v. 39, p. 125–142.

Yan, S. H., Zhang, Z. C., Wang, D. H., Chen, B. L., He, L. X., and Zhou, G., 2003, Kalatongke magmatic copper-nickel sulfide deposit, *in* Mao, J. W., Goldfarb, R. J., Seltmann, R., Wang, D, Xiao, W. J., and Hart, C., eds., Tectonic evolution and metallogeny of the Chinese Tianshan: International Association on the Genesis of Ore Deposits (IAGOD), Guidebook Series, v. 10, p. 131–152.

Yao, Y., Viljoen, M. J., Wilson, A. H., Zhong, H., Liu, B. G., Ying, H. L., Tu, G. Z., and Luo, N., 2001, Geological characteristics of PGE-bearing layered intrusions in southwest Sichuan Province, China: Economic Geology Research Unit Information Circular, no. 358, p. 1–17.

Zhang, X. S., Qin, D. X., Fan, Z. G., Hong, N., and Liu, G. L., 2005, Geochemical characters of mafic-ultramafic swarms in the Baimazhai nickel and copper deposit, Jinping, Yunnan: Geology and Prospecting, v. 41, no. 4, p. 51–56 (in Chinese with English abstract).

Zhang, X. S., Qin, D. X., Fan, Z. G., Nian, H., Liu, G. L., 2004, Genetic relation between Permian flood basalts and nickel-copper deposits in the Jinping area. Geological Prospecting, v. 40, no. 5, p. 49–56 (in Chinese with English abstract).

Zhang, Z. C., Hao, Y. L., Wang, F., and Mahoney, J. J., 2004, Petrology, mineralogy and geochemistry of the Emeishan continental flood basalts, SW China: Evidence for activity of mantle plumes: Acta Geologica Sinica, v. 78, p. 40–51.

Zhong, H., Zhou, X. H., Zhou, M. F., Sun, M., and Liu, B. G., 2002, Platinum-group element geochemistry of the Hongge Fe-Ti-V deposit in the Pan-xi area, southwestern China: Mineralium Deposita, v. 37, p. 226–239.

Zhou, T. H., Goldfarb, R. J., and Phillips, G. N., 2002, Tectonics and distribution of gold deposits in China—an overview: Mineralium Deposita, v. 37, p. 249–282.

Zhong, H., Yao, Y., Hu, S. F., Zhou, X. H., Liu, B. G., Sun, M., Zhou, M. F., and Viljoen, M. J., 2003, Trace-element and Sr-Nd isotopic geochemistry of the PGE-bearing Hongge layered intrusion, southwestern China: International Geology Review, v. 45, p. 317–382.

Zhou, M. F., Yang, Z. X., Song, X. Y., Keays, R. R., and Lesher, C. M., 2002, Magmatic Ni-Cu-PGE sulfide deposits in China, *in* Cabri, L. J., ed., The geology, geochemistry, mineralogy, and mineral beneficiation of platinum-group elements: CIM Special Volume 54, p. 619–636.

Zhou, M. F., Lesher, C. M., Yang, Z. X., Li, J. W., Sun, M., 2004, Geochemistry and petrogenesis of 270 Ma Ni-Cu-PGE sulfide-bearing mafic intrusions in the Huangshan district, eastern Xinjiang, northwest China: Implications for the tectonic evolution of the Central Asian orogenic belt: Chemical Geology, v. 209, p. 233–257.

Zhou, M. F., Wang, Y., Pang, K. N., and Shellnut, G. J., 2005, Origin of giant Fe-Ti-V oxide deposits in layered gabbroic intrusions, Pan-Xi district, Sichuan Province, SW China, *in* Mao, J. W., and Bierlein, F. P., eds., Mineral deposit research: Meeting the global challenge, v. 1: Proceedings of the 8th Biennial SGA Meeting, Beijing China, p. 511–513.

Zhu, B. Q., Dai, T. M., Hu, Y. G., Zhang, Z. W., Chen, G. H., and Peng, X. Y., 2004, The isotopic dating evidence of two periods of hydrothermal mineralization in the large igneous province of Emeishan basalts in northeast Yunnan, China: Bulletin of Mineralogy, Petrology, and Geochemistry, v. 23 (suppl.), p. 108 (in Chinese).

Zhu, B. Q., Hu, Y. G., Zhang, Z. W., and Chang, X. Y., 2003, Discovery of the copper deposits with features of the Keeweenawan type in the border area of Yunnan and Guizhou provinces: Science in China, Series D, v. 46 (suppl.), p. 60–72.